A New Liquid Crystal Color Calibration Technique Using Neural Networks and Median Filtering

Dae Hee Lee*, Jae Hun Chung, Se Youl Won
Yun Taek Kim and Kwang Suk Boo
(Inje University)

This study has developed a new liquid crystal calibration technique using Neural networks with median filtering and applied this technique to heat transfer measurements. To verify the validity of this new measurement technique, the local Nusselt numbers on a flat plate surface subjected to an axisymmetric impinging jet were measured and compared with the results by the conventional Hue-temperature calibration technique under the same conditions. Because the Neural networks predict the non-linear relations between temperatures and corresponding R, G, B values, Neural networks-median filtering calibration technique can utilize a much wider color band in the experiment than the Hue-temperature calibration technique, resulting in a significant reduction in the experimental time.

Key Words : Liquid Crystal, Neural Networks, Color Image Processing System, Median Filter, Gold Film Intrex

Nomenclature

A : Surface area of the gold film Intrex (m^2)
d : Pipe nozzle diameter (m)
f : Gold coating uniformity factor
h : Heat transfer coefficient (W/m^2K)
I : Current across the gold film Intrex
k_a : Thermal conductivity of air (W/mK)
L : Nozzle-to-surface distance (m)
L/d : Dimensionless nozzle-to-surface distance
Nu : Local Nusselt number ($=hd/k_a$)
Nu_{st} : Stagnation point Nusselt number
q_c : Conduction heat loss (W/m^2)
q_r : Radiation heat loss (W/m^2)
q_v : Convection heat loss (W/m^2)
r : Streamwise distance from the stagnation point (m)
r/d : Dimensionless streamwise distance from the stagnation point
Re : Reynolds number ($=U_{ce}d/\nu$)
T_a : Ambient temperature (℃)
T_j : Jet temperature (℃)
T_w : Wall temperature of the plate surface (℃)
U_{ce} : Jet centerline mean velocity at the nozzle exit (m/s)
V : Voltage across the gold film Intrex

Greek symbols

ε : Emissivity of the liquid crystal and black paint coated surface (measured by infra red radiation thermometer: Minolta/505s)
ν : Kinematic viscosity of air (m^2/s)
σ : Stefan-Boltzman constant (W/m^2K^4)

* Corresponding Author,
E-mail : mechdhl@ijnc.inje.ac.kr
TEL : +82-525-320-3185 ; **FAX** : +82-525-324-1723
Associate Professor, School of Mechanical and Automotive Engineering, Inje University, Kimhae Kyungnam 621-749, Korea. (Manuscript Received June 1, 1999 ; Revised October 5, 1999)

1. Introduction

Liquid crystals are substances which are in the intermediate state between the isotropic structure of liquid and the crystalline structure of solid. Thus, they have both the mechanical properties of liquid and the optical properties of solid. The array of molecules of liquid crystals is changed due to the influence of temperature, shear stress, electromagnetic field, and pressure. This variation

of the molecular array in turn changes the optical properties of liquid crystal. Liquid crystals were first observed more than 100 years ago by Friedrich Reinitzer. There are three categories of liquid crystals according to their molecular structure. They are smectic, nematic and cholesteric liquid crystals. Of these three types, cholesteric liquid crystals are the least ordered and have a delicately balanced molecular structure that can be easily upset.

The principle of the color change in the cholesteric liquid crystal lies in the helical structure of molecular array as shown in Fig. 1. This helical structure rotates due to the effect of temperature and reflects the constant light of wavelength. The cholesteric liquid crystal changes from the solid state to the liquid state with temperature and at first reflects the light of wavelength of the red color as shown in Fig. 2. As the temperature

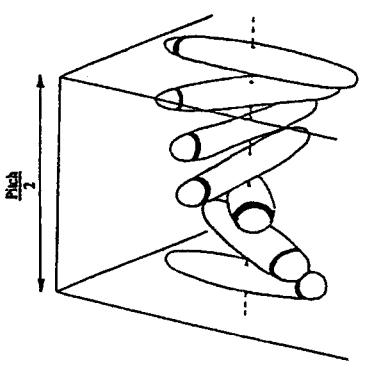

Fig. 1 The helical structure of cholesteric liquid cytstal

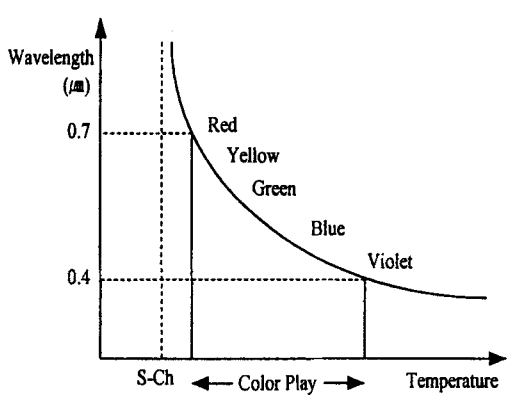

Fig. 2 Typical reflected wavelength (color)/temperature response of liquid crystal

increases, liquid crystal reflects by turns the light of wavelength within the visible ray range up to the yellow, green, blue, and violet color. The color change of liquid crystal with temperature is reversible and the color returns to its original color after the full state change. The studies of liquid crystals were confined to material laboratories before 1960's. Since Fergason(1964) reported the characteristics of liquid crystals, their usages in heat transfer applications have been widely expanded. When liquid crystals are compared with thermocouples and other temperature sensors, they have advantages of knowing the continuous color variation along with the temperature change in the wide area of the test section and visualizing the flow fields.

Cooper et al. (1975) applied the liquid crystal to the convective heat transfer study in the flow over the heated cylinder. Goldstein and Timmers (1982), Baughn and Shimizu(1989), and Lee et al.(1994, 1995, 1997) used the liquid crystal for the heat transfer measurement with circular impinging jets. Schultz and Jones(1973), and Jones(1977) reviewed the heat transfer studies using thermal paint. Also, Ireland and Jones (1985), Jones and Hippensteele(1987), Camci et al.(1991) have used liquid crystals to map the surface isotherms. Recently, the applications of liquid crystals have been on the rise in the heat transfer study, the temperature measurement, and the visualization of the temperature field. However, there exist difficulties in using the liquid crystal as a temperature sensor because it requires a highly sophisticated color calibration technique.

The present research results in the development of a color calibration technique. It turns out that the former produces the heat transfer results with lower uncertainties and is able to utilize a much wider color band of liquid crystal in the experiment, resulting in the significant time savings in the experiment without sacrificing the measurement accuracy.

It should also be noted that a sophisticated software package using C^{++} language has been developed, which can conveniently execute various tasks during the experiment from the liquid

crystal calibration to the heat transfer calculation.

2. Liquid Crystal Calibration

2.1 Calibration apparatus

In this research, the micro-encapsulated thermochromic liquid crystal (HALLCREST "R35C5W") is used for the surface temperature measurement. Since the actual color image of liquid crystal is affected by factors such as the thickness of liquid crystal, the angle, the distance and the light illuminating the liquid crystal coated surface, a careful color calibration has to be carried out under the particular conditions and later the experiments are carried out under the same conditions as those for the calibration.

Figure 3 shows a diagram of the test apparatus for liquid crystal calibration. A 170mm×75mm×50mm aluminum block was used to generate a linear temperature gradient along the length. The top hot end of the aluminum block is set by 100W cartridge heater embedded inside the block, which is operated by a DC power supply. The bottom cold end is immersed in the constant temperature water bath maintaining to within ±0.01℃ of the set temperature, generating a linear temperature gradient along the length of the aluminum block. The entire aluminum block except for the part immersed in water is completely covered by the urethane foam insulation to minimize the heat loss through its surfaces.

An air brush is used to apply the liquid crystal and black backing paint on the front surface of the aluminum block. To measure the liquid crystal surface temperature, used three 0.13 mm diameter Chromel-Constantan thermocouples fed through the back of the block and their junctions are in a good thermal contact with the liquid crystal sheet using a thermally conductive paste (OMEGA Therm). All of thermocouples were calibrated against the Platinum Resistance Thermometer (SDL CO. T25/30) which was also calibrated by NAMAS (National Measurement Accreditation Service in UK) from the temperature range of −70℃ ~420℃ to an accuracy of ±0.01℃.

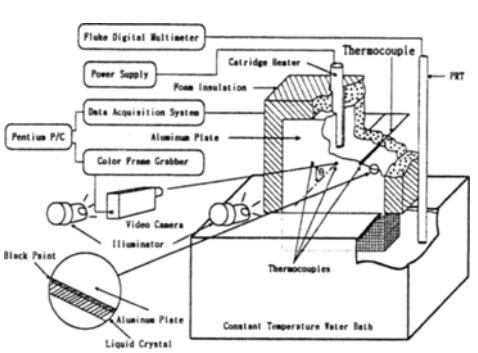

Fig. 3 Schematic diagram of the apparatus for the liquid crystal color calibration

When the temperature distributions on the liquid crystal coated surface reach the steady state, the corresponding color images are recorded by the digital color image processing system and later processed, producing a color-temperature calibration result. As shown in Fig. 3, the color image processing system consists of the color video camera(Sony/CCD-FX410), the color image grabber(Darim/Visible Office) and Pentium/PC. The Lux meter (Takemura Electric Works LTD, DM-28) is also used to measure the light intensity accurately near the aluminum block surface.

2.2 Extraction of R, G, B values

The Windows program written in C++ language has been developed. This program utilizes the Neural networks and median filtering technique in a space domain to enhance the calibration accuracy and can conveniently execute various tasks from the liquid crystal calibration to the heat transfer calculation. The distributions of R (Red), G(Green), B(Blue), H(Hue), S(Saturation), and I(Intensity) in the liquid crystal color images captured by the color CCD camera and the frame grabber are obtained using the above program.

For the liquid crystal calibration, it is assumed that there exists a one-dimensional temperature gradient in the vertical direction along the length of the aluminum block, while the temperatures are nearly isothermal along the horizontal lines upon which three thermocouples are evenly spaced for the surface temperature measurements.

Now, the average temperature for a particular

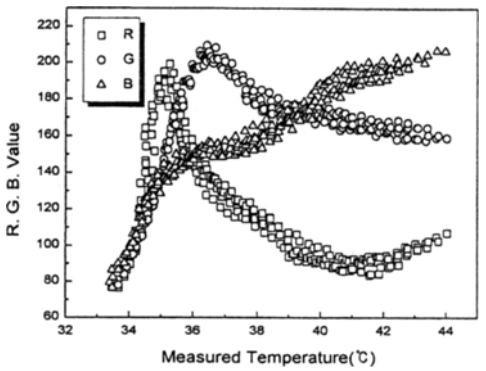

Fig. 4 Variation of R, G, B values of liquid crystal color with measured temperatures

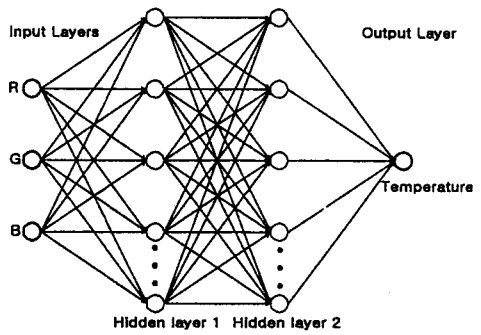

Fig. 5 The structure of Neural networks for the estimate of temperature

isothermal line is obtained using three thermocouples and corresponding R, G, B values are determined. Thus, the main idea of the median filtering technique is to determine R, G, B values by taking the average of R, G, B values corresponding to the measured temperatures along the horizontal isothermal line(i. e. unicolor line).

Figure 4 shows the distributions of the averaged R, G, B values corresponding to the measured average temperatures ranging from 35℃ to 44℃. It is observed that there exist strong non-linear relations between R, G, B values and temperatures. It is also observed that R, G, B values for the same temperature show some variations. This may be attributed to the fact that in spite of the images with the same temperature distribution being captured, digital images become corrupted with noise(called impulse noise) from the various parts of the digital color image processing system.

Now, the Neural networks with median filtering technique comes into play to compensate the non-linear relations between R, G, B values and temperatures and to remove the impulse noise and restore the corrupted images to an acceptable level.

3. The Structure and Learning of Neural Networks

The liquid crystal is expressed by R, G, B values according to temperatures and the structure of Neural networks to estimate the temperature of liquid crystal from R, G, and B values is shown in Fig. 5. Temperatures and R, G, B values are taken as output and input, respectively, in the proposed Neural networks. Thus, there are three nodes in the input layer and one node in the output layer. Besides, two hidden layers are utilized between the input and the output layer in order to equip with much higher non-linear characteristics. In doing so, the Neural networks will better predict the relations between temperatures and R, G, B values. Two hidden layers have 8 and 5 nodes, respectively. The structure of Neural Networks is very stable and has a high learning convergence due to its feed-forward multi-layer perceptron structure.

In Fig. 5, 70% of R, G, B values are randomly extracted from Fig. 4 and then are gone through the learning process and the rest 30% of R, G, B values are used to verify the appropriation of learning process. In the learning process, the generalized special learning which reduces the error is used in order to give the proper weighting factors to the nodes in the hidden layer by returning the information about the error between the predicted and the measured temperature to the hidden layers. In the learning process, the iteration rate and the momentum rate are 0.75 and 0.55, respectively.

Figure 6 shows the variation of the learning error with the number of learning iteration. The targeted learning error that decides when to stop the learning process is 0.0001. It is found from Fig. 6 that the learning fast approaches the targeted learning error at the iteration rate of 20,000. Considering the learning error is the square of

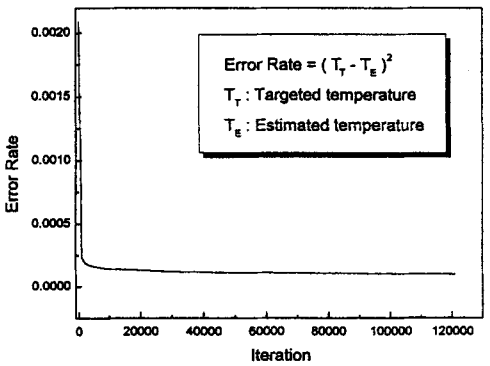

Fig. 6 Variation of learning error with the number of learning iteration in Neural networks

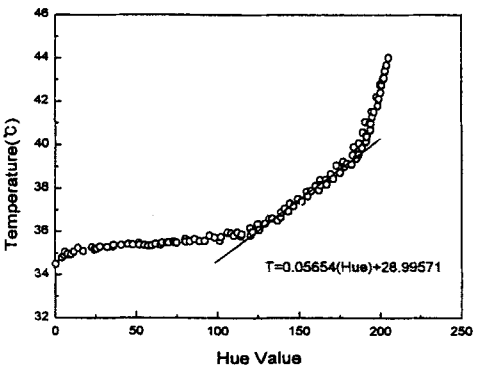

Fig. 8 Variation of the measured temperatures with Hue values

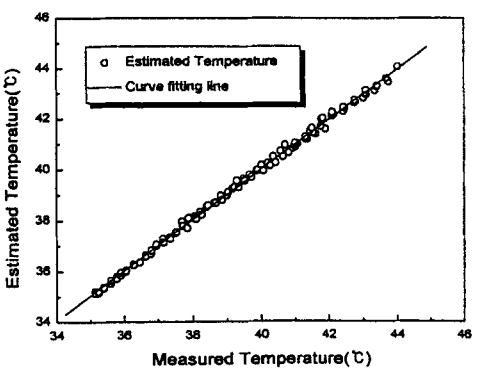

Fig. 7 Comparison between the measured temperature and the estimated temperature using Neural networks

difference between the targeted and the estimated temperature, the actual error between two temperatures is only 0.01℃, which is compatible to the error due to the thermocouple.

Figure 7 shows the comparison of the measured temperatures with the estimated ones by Neural networks. It is found that although the relations between R, G, B values and temperatures display the strong non-linear character (see Fig. 4), the estimated temperatures using Neural networks are within ±0.27℃ agreement with the measured temperatures. Besides, the usable temperature region in Fig. 7 ranges from 35℃ to 44℃, which is nearly 4℃ wider than the specified temperature range(i. e. R35C5W). These are indicative of the precision and usefulness of the calibration technique using Neural networks and median filtering. The key to success of the Neural networks and median filtering calibration technique is to compensate the non-linear character of liquid crystal colors and to remove impulse noise from the digital color image processing system.

Figure 8 shows the distribution of the measured temperatures versus Hue values of liquid crystal. It is the result of the conventional Hue-temperature calibration technique. Its working principle is to find the linear region from the Hue-temperature distribution curve and deduce the corresponding linear equation which can be used as the liquid crystal calibration equation. Figure 8 also shows that the usable linear temperature region runs from 36℃ to 39℃ with ±0.33℃ scatter from the curve fitting equation, which is almost 2℃ narrower than the specified operating temperature range of liquid crystal(i. e. R35C5W). It is concluded that the usable temperature range for the Neural networks and median filtering calibration technique is 5~6℃ wider than the conventional Hue-temperature calibration technique.

4. Application of Neural Networks to Heat Transfer Measurements

A schematic diagram of the test apparatus for the heat transfer from the flat plate to the round impinging jet is shown in Fig. 9. The apparatus consists of a blower, a heat exchanger, an orifice flow meter, a long straight pipe with an inner diameter of d=2.16cm, and a convex hemispherical surface. The development length-to-diameter

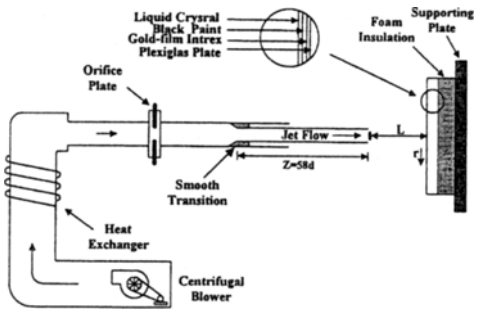

Fig. 9 Schematic deagram of the test apparatus for the impinging jet heat transfer from the flat plate

ratio of $L/d=58$ results in a fully developed flow at the nozzle exit. A heat exchanger is used to maintain the jet temperature at the nozzle exit within ± 0.2℃ of the ambient temperature. The test model consists of 5mm thick Plexiglas plate to which the gold film Intrex (a gold-coated polyester substrate sheet) of having a thickness of 1.27×10^{-4}m and an area of 5.76×10^{-2}m² is glued. An air brush is used to apply the micro-encapsulated thermochromic liquid crystal and black backing paint on the Intrex surface. A digital color image processing system is used to determine the temperature quantitatively corresponding to a particular color of liquid crystal. The measurement technique in this study, described by Lee et al. (1995, 1997), provides a method for determining the surface isotherms using the liquid crystal.

Similar to the liquid crystal calibration, the Windows program which utilizes C^{++} language is developed for the heat transfer measurements. This program not only executes liquid crystal calibration, but also carry out various tasks such as calculation of the local and average Nusselt numbers, etc.

By heating a very thin gold coating on the Intrex electrically, an uniform wall heat flux condition is established. The heat flux can be adjusted by changing the current through the Intrex, which changes the surface temperature. Under the constant heat flux condition, an isotherm on the Intrex surface corresponds to a contour of a constant heat transfer coefficient. The local heat transfer coefficient at the position of the particular color being observed is calculated from

$$h=q_v/(T_w-T_j) \tag{1}$$

where the net heat flux q_v is obtained by subtracting the heat losses from the total heat flux through the Intrex; i. e.

$$q_v=fIV/A-\varepsilon\sigma(T^4{}_w-T^4{}_a)-q_c \tag{2}$$

The ratio of the local electrical heating to the average heating, f, is a measure of the uniformity of the gold coating on the Intrex. Baughn et al. (1989b) found the uniformity to be as high as 98% when the test section of the Intrex is small and selected from the middle of a roll where the gold-coating is most uniform, which has been the case for the present experiment. Therefore, we assume $f\approx 1$ for the heat flux calculation, but f is maintained in equation (2) because it contributes to the overall Nusselt number uncertainty (Table 1). The condition loss, qc, through the back of the plate is small compared to the surface heating and is assumed to be zero. However, it is included in the equation because it also contributed to the overall Nusselt number uncertainty.

Table 1 Nusselt number uncertainty analysis

Xi	Value	δ Xi	$\left(\frac{\partial X_i}{Nu}\frac{\partial Nu}{\partial Xi}\right)\times 100(\%)$	
			r/d=0	5.09
T_w	35.5(℃)	0.30	2.15	2.14
f	1	0.02	2.00	2.00
T_i	21.5;21.4(℃)	0.15	1.04	0.95
q_c	0(W/m²)	22.17;6.55	0.97	0.89
V	34.88;19.48(V)	0.125	0.36	0.64
I	3.79;2.17(A)	0.01	0.26	0.46
d	2.16(cm)	5.0×10^{-3}	0.22	0.23
ε	0.9	0.05	0.19	0.60
A	0.0576(m²)	5.0×10^{-5}	0.09	0.09
Total Nu uncertainty		$\delta Nu/Nu=3.31$		3.36

The uncertainty analysis has been carried out using the method by Kline and McKlintock (1953). Table 1 shows that the Nusselt number uncertainty for $L/d=6$, $r/d=0$ and $r/d=5.09$ at $Re=23{,}000$ is 3.31% and 3.36%, respectively. It should be noted that this uncertainty represents the maximum uncertainty in the Nusselt number

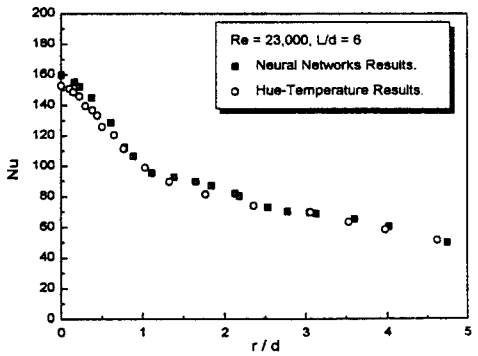

Fig. 10 Comparison of the Neural networks results with Hue-temperature results

under the given experimental conditions. The uncertainty in the wall temperature of the plate surface is the largest contribution to the overall Nusselt number uncertainty. Another important source of uncertainty is the gold coating uniformity. The present uncertainty estimates are based on 20:1 odds (i. e. 95% confidence level of both the precision and bias errors).

5. Discussion of Results

Figure 10 shows a comparison between the heat transfer results by the conventional Hue-temperature calibration technique and those by Neural networks with median filtering. It is found that in the entire region, Nusselt numbers measured by Neural networks with median filtering agree within $\pm 4.4\%$ with those by the Hue-temperature calibration technique.

The Hue-temperature calibration technique uses only the linear region in the Hue-temperature distribution curve so that the usable region is only about 60% of the specified color band width of liquid crystal. But the Neural networks-median filtering calibration technique can expand the usable range of liquid crystal beyond the specified color band width and can significantly save the experimental time without sacrificing an accuracy. Thus, the new liquid crystal calibration technique using the Neural networks and median filtering proves to be accurate and very useful.

6. Conclusions

A new liquid crystal calibration technique using Neural networks with median filtering has been developed and applied to heat transfer measurements. To verify the validity of this new measurement technique, the local Nusselt numbers on a flat plate surface subjected to an axisymmetric impinging jet were measured and compared with the previous experimental results using the conventional Hue-temperature calibration technique. Because Neural networks predict the non-linear relations between temperatures and corresponding R, G, B values of liquid crystal color, the new calibration technique using the Neural networks with median filtering can utilize a much wider color band in the experiment than the Hue-temperature calibration technique, resulting in a significant reduction in the experimental time.

Acknowledgements

The authors are grateful for the support of this research by the Korea Science and Engineering Foundation through Grant No. (KOSEF:97-0220 -06-01-3).

References

Baughn, J. W., and Shimizu, S., 1989, "Heat Transfer Measurement From as Surface With Uniform Heat Flux and an Impinging Jet," *ASME Journal of Heat Transfer*, Vol. 111, pp. 1096～1098.

Baughn, J. W., Ireland, P. T., Jones, T. V., and Saniei, N., 1989b, "A Comparison of the Transient and Heated-Coating Methods for the Measurements of the Local Heat Transfer Coefficients on a Pin Fin," *ASME Journal of Heat Transfer*, Vol. 111, pp. 877～881.

Camci, C., Kim, K., Hippensteele, S. A., and Poinsatte, P. E., 1991, "Convection Heat Transfer at the Curved Bottom Surface of a Square to Rectangular Transition Duct Using a New Hue Capturing Based Liquid Crystal Technique,"

Fundamental Experimental Measurements in Heat Transfer, ASME HTD-Vol. 179.

Cooper, T. E., Field, R. J., and Meyer, J. F., 1975, "Liquid Crystal Thermography and Its Application to the Study of Convective Heat Transfer," *ASME Journal of Heat Transfer*, Vol. 97, pp. 1857~1868.

Fergason, J. L., 1964, "Liquid Crystal," *Scientific American*, Vol. 222, pp. 76~85.

Goldstein, R. J., and Timmers, J. F., 1982, "Visualization of Heat Transfer from Arrays of Impinging Jets," *International Journal of Heat and Mass Transfer*, Vol. 25, pp. 1857~1868.

Ireland, P. T., and Jones, T. V., 1985, "The Measurement of Local Heat Transfer Coefficients in Blade Cooling Geometries," *AGARD Conference Proceedings* No. 390, Paper 28.

Jones T. V., 1977, "Heat Transfer, Skin Friction, Total Temperature and Concentration Measurements," *Measurements of Unsteady Fluid Dynamic Phenomena*, Richards B. E., ed., McGraw Hill, pp. 63~102.

Jones, T. V., and Hippensteele, S. A., 1987, "High-Resolution Heat-Transfer Coefficient Maps Applicable to Compound Curve Surfaces Using Liquid Crystals in a Transient Wind Tunnel," *Development in Experimental Technique in Heat Transfer and Combustion*, ASME HTD -71.

Kline, S. J., and McKlintock, F. A., 1953, "Describing Uncertainties in Single Sample Experiments," *Mechanical Engineering*, Vol. 75, pp. 3~8.

Lee, S. J., Lee, J. H., and Lee, D. H., 1994, "Heat Transfer Measurement Using Liquid Crystal with an Elliptic Jet Impinging upon the Flat Surface," *International Journal of Heat and Mass Transfer*, Vol. 37, pp. 967~976.

Lee, D. H., and Greif, R., Lee, S. J., and Lee, J. H., 1995, "Heat Transfer from a Surface to a Fully Developed Axisymmetric Impinging Jet," *ASME Journal of Heat Transfer*, Vol. 117, pp. 772~776.

Lee, D. H., Chung, Y. S., and Kim, D. S., 1997, "Turbulent Flow and Heat Transfer Measurements on a Curved Surface with a Fully Developed Round Impinging Jet," *International Journal of Heat and Flow*, Vol. 18 No. 1, pp. 160 ~169.

Schultz, D. L., and Jones, T. V., 1973, "Heat Transfer Measurements in Short Duration Hypersonic Facilities," *Agardograph* No. 165.